

Analysis of Silicon Chip Interferometric for Bio-Sensing Application

¹ Ramya M, ² Dr.Nagaraj.R, ³ Bilkish Mondal, ⁴ Chandana B.

^{1,3,4} Student, Dept. Of ECE, The Oxford College of Engineering, Bangalore-560068.

² Principal, The Oxford College of Engineering, Bangalore-560068.

Abstract- Technologies have been developed based on silicon chips that use a thin silicon dioxide film to form a common path on chip interferometer [10-12]. The advantage of silicon chip interferometric techniques is that the glass surface chemistries developed for the well-established fluorescent microarrays may be used. In this paper, we have presented the analysis of interferometer consisting of a thin layer of gold embedded in a silicon membrane. By using FullWAVE tool from R-Soft®. From the results it is clear that interferometer consisting of a thin layer of gold embedded in a silicon membrane is highly sensitive at resonant wavelength range 1.615µm-1.625µm.

Keywords- Interferometer, SPR, Full WAVE.

1. Introduction

Using interference as a means to detect refractive index changes is not new, and integrated sensors using this principle have been realized in low-index [1] and high-index material systems [2]. Their working principle is based on the fact that refractive index variations induce a phase-shift in one of the arms of the Mach-Zehnder interferometer (MZI), this phase-shift results in an intensity variation in the output waveguide.

$$I \propto [1 + V \cos(\Delta\phi)] \dots \dots (1)$$

Where $\Delta\phi = (\phi_r - \phi_s)$ is the phase shift between guided modes in the sensing arm and the reference arm. The visibility factor (V) gives the contrast between the maximum and the minimum transmitted intensity and depends on the coupling factor of the divisor and the propagation losses of guided modes in the interferometer arms. The same principles can be applied to a surface plasmon interferometer. Design of our device is depicted in Fig. 1. The interferometer consists of a gold layer (refractive index taken from [3]) embedded into the silicon membrane (n=3.45) on top of a supporting silica layer (n=1.45).

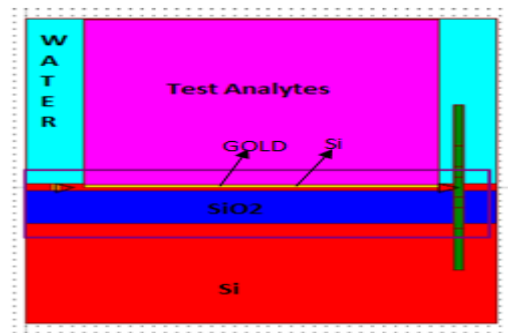


Fig1. Surface plasmon interferometer consisting of a thin layer of gold embedded in the silicon membrane

The high degree of asymmetry associated with the gold layer (top interface $n \approx 1.33$, bottom interface $n = 3.45$) assures that the surface plasmon modes associated with the upper and lower of the metal-dielectric interfaces will never be able to couple, their wave vectors differ too much. So the gold layer possesses two distinct surface-plasmon modes which propagate through the structure without influencing each-other. Exciting these modes is done by end-fire coupling from a regular SOI waveguide with the transverse-magnetic ground mode [4, 5]. At the end of the gold layer both surface plasmon mode excite the ground mode of the SOI waveguide, depending on the relative phase of the surface plasmon modes their contributions to the ground mode will interfere constructively or destructively.

2. Surface Plasmon Resonance

The use of surface plasmon resonance (SPR) for biological and chemical sensing is well established [6]. The high sensitivity of this technique to surface phenomena makes it ideal for use in real-time and label-free biosensors where very small changes in refractive index must be detected. In the past decade, several integrated optical SPR sensors have been demonstrated [7, 8, and 9], in which thin gold films

serving as a plat-form for the attachment of sensing films are deposited on top of an integrated optical waveguide system. In this paper, we analyze the interferometer consisting of a thin layer of gold embedded in the silicon membrane. We define a set of design parameters that allow tuning the operation of our sensor to a desired wavelength range and or to a desired range of analyte refractive indices.

3. FullWAVE (R-Soft)

Simulation is done by using FullWAVE R-Soft. FullWAVE uses the finite difference time domain (FDTD) algorithm. The simulation domain has been chosen to include the gold plate, as well as some of the SOI waveguide on the top and bottom of the plate. It also includes part of the device above and below the gold plate so that the extents of the two plasmon modes are included. Two physical parameters are required in order to perform a FullWAVE simulation: the material parameters, including the relative permittivity $\epsilon(r,\omega)$ and relative permeability $\mu(r,\omega)$ as a function of space and/or frequency, and the electromagnetic field excitation. In order to use the FDTD algorithm to study the propagation of light fields in a structure, the material parameters must be specified. FullWAVE utilizes the following formulas to specify the material properties of a waveguide.

$$D = \epsilon_0 E + P \dots (2)$$

$$B = \mu_0 H + M \dots (3)$$

where P and M are the polarization and magnetization can be, dispersive, non-linear, and anisotropic. Material profile has been calculated for Gold (Au) in Fig2.

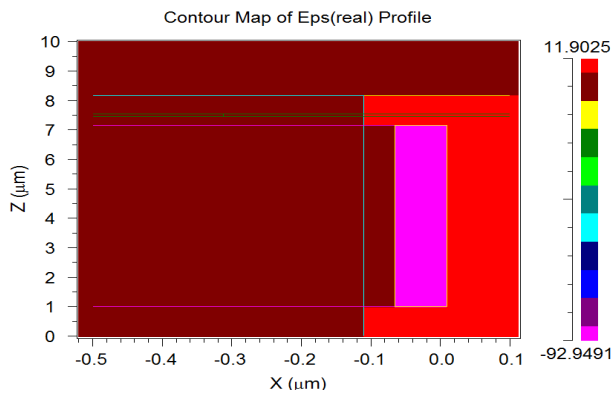


Fig2. Contour Map of material profile along Z-direction

Material dispersion, or the change of refractive index as a function of wavelength also shown in below Fig3. Operating wavelength in the range of $1.50\mu\text{m}$ - $1.60\mu\text{m}$.

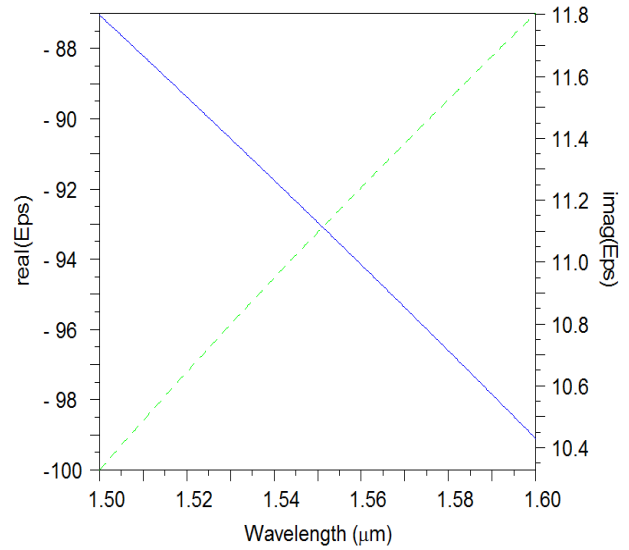


Fig3.1Eps (Real & Imag)

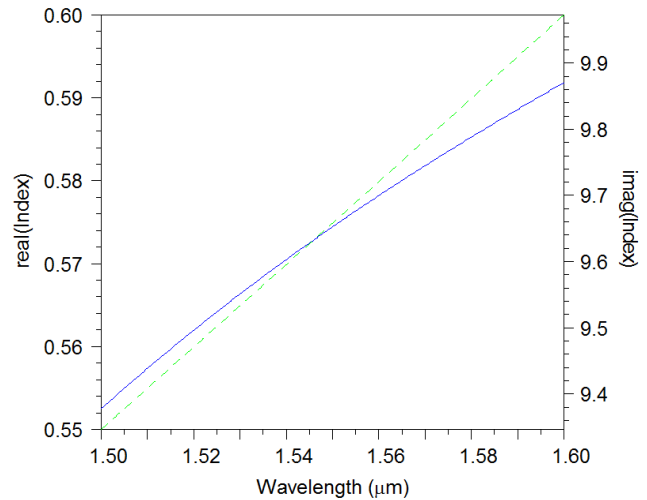


Fig3.2Refractive index of Au (Real & Imag) Vs Wavelength

Above Fig3.1-3.2 shows the dispersion relation. An initial launch condition ϕ_L at time $t=0$ is needed, as well as a driving function in time. This consists of both a spatial and temporal excitation, such as,

$$\phi_L(r,t) = f(r_0)g(t) \dots (4)$$

where $f(r_0)$ is the spatial excitation at the launch plane and $g(t)$ is the temporal excitation. A field source has been considered as gaussian along a plane in the simulation domain. Surface plasmon effect can be seen on the top of the gold (Au) plate.

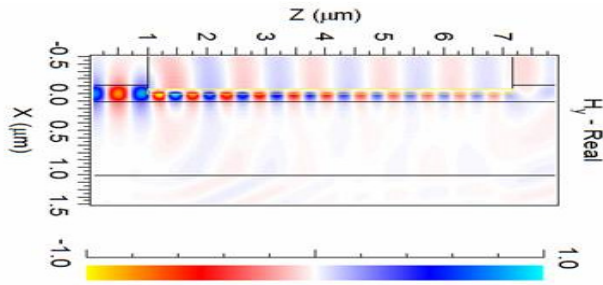


Fig4. Contour Map of the Hy component are shown. The plasmon modes are clearly seen on both sides of the gold plate

where test analytes are attached to the gold plate which is (Test_Analytes=1.3) shown in Fig4. The boundary conditions at the spatial edges of the computational domain is the perfectly matched layer (PML), in which both electric and magnetic conductivities are introduced in such a way that the wave impedance remains constant, absorbing the energy without inducing reflections. In Fig5, the intensity enhancement is depicted as a function of the angle of incidence of incoming light for a number of different thicknesses of a gold layer.

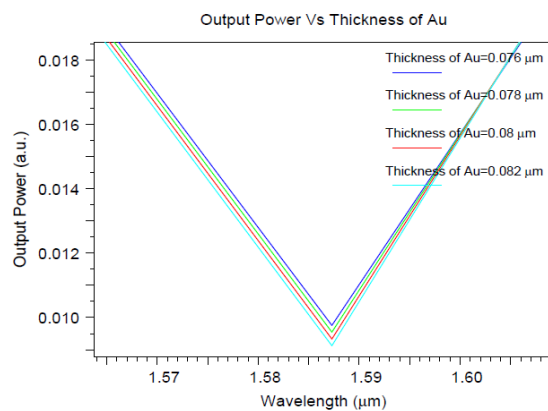


Fig5. Output power Vs Thickness of Au at the resonance wavelength 1.586μm

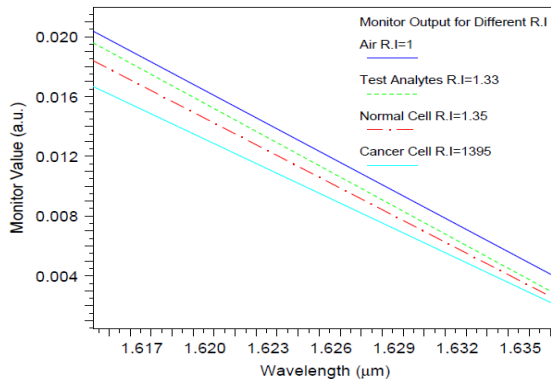


Fig6. correlation between the test refractive index and the output power

Above Fig6. shows how the quantity of the material to be measured changes the refractive index can be used to correlate the output power to the quantity to be measured. In Fig6. Simulation has been done using various various refractive index.

4. Application of Silicon Chip

Development of label-free biosensors that can simultaneously monitor multiple molecular interactions is of great interest to biomedical research and clinical applications. Detection of DNA–DNA, DNA–protein, and antibody–antigen interactions has been established using fluorescent microarrays.

5. Conclusion

Test analyte is added to the gold (Au) layer. Observation has been made out that the increment in the thickness of gold (Au), decreases the magnetic intensity amplitude. So, the incident light will have less power to simulate the thickness of gold layer to produce the surface plasmon resonance effect. Also observation has been made out that difference in the test analyte refractive index of normal cell and cancerous cell relatively changes in the output power wherein the received output power for normal cell is 0.0195 and for cancerous cell is 0.0165. It has been observed that for the wavelength 1.615μm, there is distinct shift in the output power. So it can be concluded that sensitivity of sensor in the wavelength range 1.615μm-1.625μm is very high.

References

- [1] Luff B, Wilkinson J, Piehler J, Hollenbach U, Ingenhoff J and Fabricius N, " Integrated Optical Mach-Zehnder Biosensor," J. Lightwave Technol., 16, 583-592 (1998)
- [2] Prieto F, Sepúlveda, Calle A, Llobera A, Domínguez C, Abad A, Montoya A and Lechuga L M, "An Integrated Optical Interferometric Nanodevice based on Silicon Technology for Biosensor Applications," Nanotechnology, 14, 907-912 (2003)
- [3] Handbook of Optical Constants of Solids ,edited by E. Palik, Academic Press New York (1985)
- [4] Nikolajsen T, Leosson K, Salakhutdinov I and Bozhevolnyi S, "Polymer-based Surface-Plasmon-Polariton Stripe Waveguides at Telecommunication Wavelengths," Applied Physics Letters, 82, 668-670 (2003).
- [5] S.M.Verulkar and M.Limkar. Real Time Health Monitoring Using GPRS Technology. International Journal of Computer Science and Network (IJCSN),1, 2012.
- [6] Hochberg M, Baehr-Jones T, Walker C and Scherer A, "Integrated Plasmon and Dielectric Waveguides," Opt. Express, 12 5481-5486 (2002)

- [7] Homola J, "Present and Future of Surface Plasmon Resonance Biosensors," Anal. Bioanal. Chem., 377, 528-539 (2003)
- [8] ˇCtyrock´y J., Homola J, Lambeck PV, Musa S, Hoekstra HJWM, Harris RD, Wilkinson JS, Usievich B, Lyndin NM, "Theory and Modelling of Optical Waveguide Sensors Utilising Surface Plasmon Resonance," Sens. Actuators B, 54, 66 - 73 (1999)
- [9] Harris Rd, Wilkinson JS, "Waveguide Surface Plasmon Resonance Sensors," Sens. Actuators B, 29, 261 - 267 (1995)
- [10] Homola J, ˇCtyrock´y J, Skalsk´y M, Hradilov´a J and Kol´a'rov´a P, "A Surface Plasmon Resonance Based Integrated Optical Sensor," Sens. Actuators B, 38-39, 286 - 290 (1997)
- [11] Zhao, M., Wang, X. F., Nolte, D. D., Molecular interferometric imaging. Opt. Express 2008, 16, 7102–7118.
- [12] Bergese, P., Cretich, M., Oldani, C., Oliviero, G. et al. Advances in parallel screening of drug candidates. Curr. Med. Chem. 2008, 15, 1706–1719.
- [13] Lu, J. H., Strohsahl, C. M., Miller, B. L., Rothberg, L. J., Reflective interferometric detection of label-free oligonucleotides. Anal. Chem. 2004, 76, 4416–4420.



Bilkish Mondal was born in Phulbari, West Garo Hills, Meghalaya on 8th November, 1990. She received BE (Electronics & Communication) degree from Visvaswara Technological University in 2012 from Ghousia College Of Engineering, Ramanagaram, Bengaluru, Karnataka . Presently She is a M.Tech 4th sem student from The Oxford College Of Engineering, Bangalore under VTU.



Chandana B was born in Tumkur, karnataka on 14th October, 1989. She received BE (Electronics & Communication) degree from Visvaswara Technological University in 2012 from Channabasaveshwara Institute of Technology, Tumkur, Karnataka . Presently She is a M.Tech 4th sem student from The Oxford College Of Engineering, Bangalore under VTU.

Authors Details



Ramya M, was born in Kollegal, Karnataka on 11th November, 1989. She received BE (Electronics & Communication) degree from Visvaswara Technological University in 2012 from Maharaja Institute of Technology, Mysore, Karnataka. Presently She is a M.Tech 4th sem student from The Oxford College Of Engineering, Bangalore under VTU.



Dr. Nagaraj Ramrao, is The Principal, The Oxford College of Engineering, Bangalore, Karnataka, India. He has obtained doctoral degree from the VTU for a thesis on Automatic Flight Control. His research interests are Aerospace Electronics, Industrial Electronics & Control and Digital Signal Processing. He has guided more than 50 undergraduate Projects & Post graduate Projects. He is also guiding a

number of Ph.D scholars.